



Supplementary Information for
GPCR large-amplitude dynamics by ^{19}F -NMR of aprepitant bound
to the neurokinin 1 receptor

Benxun Pan^{a,b,c,d}, Dongsheng Liu^a, Lingyun Yang^a, Kurt Wüthrich^{a,e}

^aHuman Institute, ShanghaiTech University, Shanghai 201210, China.

^bSchool of Life Science and Technology, ShanghaiTech University, Shanghai 201210, China.

^cCAS Center for Excellence in Molecular Cell Science, Shanghai Institute of Biochemistry and Cell Biology, Chinese Academy of Science, Shanghai 201210, China.

^dUniversity of Chinese Academy of Sciences, Beijing 100049, China.

^eDepartment of Integrative Structural and Computational Biology, Scripps Research, La Jolla, CA 92037, USA.

*Kurt Wüthrich

Email: wuthrich@shanghaitech.edu.cn; wuthrich@scripps.edu

This PDF file includes:

Supplementary text

Figures S1 to S11

Tables S1

SI References

Supplementary Information Text

Protein Expression in *Pichia pastoris*. The gene encoding the polypeptide of residues 2–335 of human NK1R contained an N-terminal α -factor leader peptide, a FLAG tag (DYKDDDD), a BRIL fusion protein, a PreScission Protease (PPase) cleavage site, a tobacco etch virus protease (TEV) cleavage site and a C-terminal 10×His tag (Fig. S1A). This construct was cloned into a pPIC9K vector and introduced by electroporation into the Bg12 strain of *Pichia pastoris* (BioGrammatics, Carlsbad, CA). The colony selection and protein expression followed previously published protocols (1, 2). Briefly, the transformed cells were spread onto yeast nitrogen base (YNB) plates and allowed to grow for 2 to 3 days at 30 °C. Twenty colonies were randomly selected for inoculation of 4 mL samples of buffered minimal glycerol (BMGY) medium, which were then grown for two days at 30 °C. Cells were transferred into 4 mL buffered minimal methanol (BMMY) media by centrifugation. Cells were harvested by centrifugation after addition of 0.5% (w/v) methanol and shaken at 27 °C for 36 hours with a 12-hour interval. Each colony was tested by anti-His Western blot, and four of them were further compared at larger scale of 500 mL cultures by using aSEC. Finally, the best expression colony was used for protein expression and purification in this study.

Protein Expression in Insect Cell System. The human NK1R gene (2–335) containing the mutation E78^{2.50}N and fused with mT4L between S226 and H237, was cloned into a pFastBac HTA vector that contains an expression cassette with haemagglutinin signal sequence (HA), Flag tag, and deca-histidine tag. A PPase site was inserted between His tag and NK1R gene (*SI Appendix*, Fig. S2A). The Bac-to-Bac Baculovirus Expression System (Invitrogen) was used to generate high-titer recombinant baculovirus ($>10^9$ viral particles per mL). Recombinant baculovirus was produced by transfecting recombinant bacmids (2.5–5 mg) into *Spodoptera frugiperda* (*Sf9*) cells (2.5 mL, density of 1×10^6 cells per mL). After 4 days of shaking at 27 °C, P0 viral stock was harvested as the supernatant of the cell suspension to produce high-titer viral stock. Viral titers were analyzed by flow cytometry on cells. NK1R was expressed by infecting *Sf9* cells at a cell density of $2\text{--}3 \times 10^6$ cells per mL with P1 virus at a

multiplicity of infection of 5. Finally, cells were harvested by centrifugation at 48 hours post-infection and stored at $-80\text{ }^{\circ}\text{C}$.

Preparation of NK1R Reconstituted in Micelles. Yeast cells were disrupted with a high-pressure cell disruptor (JN BIO, Guangzhou) at 1,800 bar with circulating cold water at $4\text{ }^{\circ}\text{C}$. Cell debris were separated from the membrane suspension by 4,500 rpm centrifugation for 10 minutes. The solution was further centrifugated at 35,000 rpm for 40 minutes, then the pelleted membranes were washed with high-salt buffer. The purified membranes were then resuspended in the low-salt buffer with $100\text{ }\mu\text{M}$ aprepitant, 2 mg/mL iodoacetamide, protease inhibitor (TargetMol, USA), and incubated at $4\text{ }^{\circ}\text{C}$ for 1 hour. The membranes were then solubilized in 50 mM HEPES (pH 7.5), 0.5% (w/v) DDM, 0.1% (w/v) CHS and 500 mM NaCl. After incubation at $4\text{ }^{\circ}\text{C}$ for 6 hours, the supernatant was isolated by ultracentrifugation at $35,000\text{ rpm}$ for 30 minutes. The soluble fraction was supplemented with 30 mM imidazole and incubated with TALON Superflow high-affinity resin (Clontech) overnight at $4\text{ }^{\circ}\text{C}$.

The resin was washed with 20 column volumes of wash buffer containing 20 mM HEPES (pH 7.5), 0.05% (w/v) DDM, 0.01% (w/v) CHS, 500 mM NaCl, and 30 mM imidazole, and then incubated in a LMNG exchange buffer containing 20 mM HEPES (pH 7.5), 0.5% (w/v) LMNG, 0.1% (w/v) CHS, 300 mM NaCl, and 30 mM imidazole for 2 hours. The resin was further washed by buffer containing 20 mM HEPES (pH 7.5), 0.01% (w/v) LMNG, 0.002% (w/v) CHS, 300 mM NaCl, and 30 mM imidazole for 20 column volume. The NK1R sample was then eluted with elution buffer containing 20 mM HEPES (pH 7.5), 0.01% (w/v) LMNG, 0.002% (w/v) CHS, 300 mM NaCl and 300 mM imidazole.

The receptors were concentrated to about 0.5 mL with a 50 kDa molecular weight cut-off concentrator and exchanged with NMR buffer (20 mM HEPS (pH 7.5), 0.01% (w/v) LMNG, 0.002% (w/v) CHS, 100 mM NaCl). Peptide-*N*-glycosidase F (PNGase F) was used to remove the potential glycosylation. The sample was subsequently passed through HiTrap™ Q 1 mL column for further purification. The purified NK1R-aprepitant complexes were concentrated to $400\text{ }\mu\text{L}$ and supplemented with $20\text{ }\mu\text{M}$ trifluoromethylacetic acid (TFA), $50\text{ }\mu\text{M}$

2,2-dimethyl-2-silapentane-5-sulfonic acid (DSS) and 40 μ L D₂O. NK1R[2–335] reconstituted in LMNG/CHS micelles was assessed by SDS-PAGE and aSEC using Sepax Nanofilm SEC-250 column, which showed high homogeneity of the protein sample (*SI Appendix*, Fig. S1, B and C). For NMR data acquired in DDM/CHS, proteins were purified with the DDM/CHS instead of LMNG/CHS. The protein yield from 1 L *Pichia pastoris* culture were about 1.0 mg for NK1R[2–335] and 4.0 mg for NK1R[2–335, E78^{2.50}N], respectively.

NK1R[2–335, E78^{2.50}N]–mT4L expressed in insect cells was purified as previously described (3). The cells were disrupted by thawing frozen cell pellets in a low-salt buffer and by dounce homogenization. The membrane was washed by repeating centrifugation and homogenization in high-salt buffer twice. Purified membrane was extracted by adding solubilization buffer containing 50 mM HEPES (pH 7.5), 0.5% (w/v) DDM, 0.1% (w/v) CHS and 500 mM NaCl and incubating at 4 °C for 3 hours. After centrifugation, the supernatant was supplemented with 30 mM imidazole and incubated with TALON Superflow high-affinity resin (Clontech) overnight at 4 °C. The protein was then purified by IMAC method as described for the protein expressed in yeast.

Preparation of the Membrane Scaffold Protein MSP1D1. MSP1D1 was expressed and purified as previously described (4). The *Escherichia coli* BL21 (DE3) strain transformed with the plasmid encoding His-tagged MSP1D1 was cultured at 37 °C in Terrific Broth (TB) medium containing 100 mg/L of kanamycin. When the culture reached an OD₆₀₀ of 0.6, 1 mM of isopropyl- β -D-thiogalactoside (IPTG) was added to induce protein expression. The culture was continuously shaken at 37 °C for 3 hours. The cells were harvested by centrifugation at 5,000 rpm for 15 minutes, and the resultant cell pellets were stored at –80 °C until use. The cells were suspended in buffer A containing 20 mM phosphate (pH 7.4), 300 mM NaCl, deoxyribonuclease I, 1% Triton X-100 and disrupted by sonication. The cell lysate was centrifuged at 20,000 rpm for 30 minutes. The supernatant was loaded to Ni-NTA agarose, and the resin was washed with 20 column volumes of buffer B containing 40 mM Tris/HCl (pH 8.0), 300 mM NaCl and 1% Triton X-100, and then washed with buffer C containing 40 mM

Tris/HCl (pH 8.0), 300 mM NaCl, 50 mM sodium cholate, and 20 mM imidazole. The resin was further washed with buffer D containing 40 mM Tris/HCl (pH 8.0), 300 mM NaCl, and 50 mM imidazole. The His-tagged MSP1D1 was eluted with buffer D supplemented with 300 mM imidazole. Finally, the TEV protease was added to the eluate to remove the His-tag, and the reaction mixture was dialyzed against 20 mM Tris/HCl (pH 8.0) and 100 mM NaCl. After 12 hours of cleavage, the reaction mixture was reloaded to the Ni-NTA agarose column. The flow-through was collected and concentrated for reconstitution of NK1R.

Reconstitution of NK1R into Nanodiscs. Purified NK1R[2–335] was mixed with MSP1D1, 1-palmitoyl-2-oleoyl-glycero-3-phosphocholine (POPC, Sigma) and 1-palmitoyl-2-oleoyl-sn-glycero-3-phospho-L-serine sodium salt (POPS, Sigma) at a molar ratio of NK1R:MSP1D1:(POPC/POPS) = 1:5:350. The ratio of POPC to POPS was 7:3 (4). The cholate concentration was adjusted to 12–40 mM by adding 200 mM sodium cholate in 20 mM phosphate (pH 7.4) and 150 mM NaCl. After 1-hour incubation at 4 °C, 0.5 g SM-2 Bio-Beads (Bio-Rad) were added, and the mixture was further incubated overnight at 4 °C. The empty nanodiscs were removed by passing through the Ni-NTA agarose column. The NK1R nanodiscs bound to the beads were eluted with 20 mM phosphate (pH 7.4), 150 mM NaCl, and 300 mM imidazole. The eluate was concentrated to about 500 µL and loaded to a Superdex 200 Increase 10/300 GL column for further purification. The fractions from 12.5–16.2 ml were collected and concentrated for NMR measurements (*SI Appendix*, Fig. S1, *E* and *F*).

NMR Spectroscopy. ¹⁹F-chemical shifts were referenced using an internal standard of TFA at –75.5 ppm. 1D ¹⁹F-NMR experiments were recorded with a data size of 4,096 complex points, an acquisition time of 90 ms, and 2,048 scans per experiment. Saturation transfer ¹⁹F-NMR experiments were recorded with the same data size and 512 scans per experiment. 2D [¹⁹F, ¹⁹F]-EXSY experiments were recorded with a data size of 1,024 and 36 complex points in the direct and indirect dimensions, respectively; 1,024 scans were accumulated per increment. The data were analyzed by using the software MestReNova version 12.0.3 (Mestrelab

Research S.L.). Saturation transfer data were fitted with equation (3) in *SI Appendix* by software OriginPro 2019 (OriginLab).

Measurement of T_1 by Inversion-recovery Experiments. The longitudinal spin relaxation times of ^{19}F signals, T_1 , were determined using the inversion–recovery experiment as implemented in the standard Bruker pulse program library (t1ir) (*SI Appendix* Figs. S4 and S6). The sample concentration was 200 μM . Twelve experiments with delays of 0.001, 0.05, 0.10, 0.20, 0.50, 0.80, 1.00, 1.50, 2.00, 3.00, 5.00, and 8.00 s were recorded, using a recycle delay (d1) of 3.00 s and accumulation of 512 scans per increment. 2048 complex points were recorded with an acquisition time of 85 ms.

T_1 was determined by fitting the peak intensities with the function $I_t = I_0 * [1 - 2 * \exp(-t/T_1)]$, where t is the variable delay in the pulse sequence, using the software Dynamics Center version 2.5.3 (Bruker BioSpin). The fitting errors were estimated by Monte Carlo simulations.

Calculation of Exchange Rates by Analysis of 2D [^{19}F , ^{19}F]-EXSY Spectra. The exchange rate k_{ex} was calculated from the 2D [^{19}F , ^{19}F]-EXSY spectra with the equations (5):

$$k_{ex} = \frac{1}{\tau_m} \ln \frac{r+1}{r-1} \quad (1)$$

$$r = \frac{4p_1p_2(I_{11}+I_{22})}{I_{12}+I_{21}} - (p_1 - p_2)^2 \quad (2)$$

I_{11} and I_{22} represent the intensities of diagonal peaks, I_{12} and I_{21} represent the intensities of cross peaks, p_1 and p_2 are the populations of states 1 and 2, respectively.

Calculation of Exchange Rates by Analysis of Saturation Transfer Spectra. The saturation transfer experiments were analyzed on the basis of the solutions of the Bloch–McConnell equations (6,7), using the approximation that $T_2 \ll T_1$. The exchange rate, k_{AB} , between states A and B can be determined by the response of A, if the pre-irradiation was applied at B.

$$M_t^A = M_0^A \left\{ \frac{k_{AB}}{R_{1A} + k_{AB}} \exp[-t(R_{1A} + k_{AB})] + \frac{R_{1A}}{R_{1A} + k_{AB}} \right\} \quad (3)$$

where R_{1A} represents the longitudinal spin relaxation rate at site A.

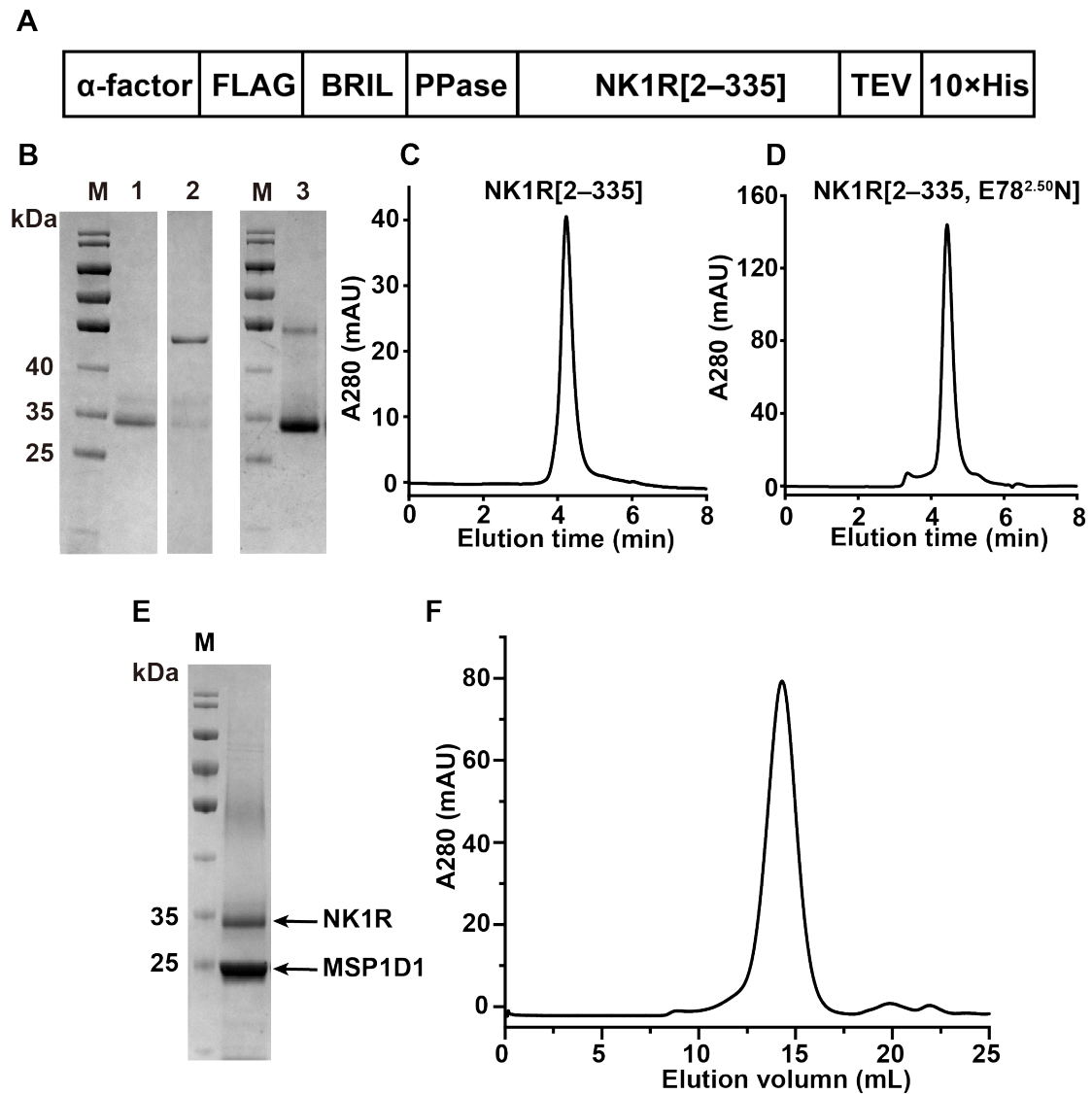


Fig. S1. NK1R[2–335] expression in *Pichia pastoris* for NMR sample preparation in detergent micelles and nanodiscs. (A) NK1R[2–335] construct used for yeast expression; it includes the leader sequence α -factor, a FLAG tag sequence, the fusion protein BRIL, the protease recognition site (PPase), NK1R[2–335], the tobacco etch virus protease recognition site (TEV) and a C-terminal 10 \times His tag. (B) SDS-PAGE of purified NK1R. Lanes 1 and 2: NK1R[2–335] after and before PPase digestion. Lane 3: NK1R[2–335, E78^{2.50}N] after PPase digestion. (C) and (D) aSEC of NK1R[2–335] and NK1R[2–335, E78^{2.50}N] in complex with the antagonist apreptant in LMNG/CHS mixed micelles using Sepax Nanofilm SEC-250 column. (E) SDS-PAGE of NK1R[2–335] reconstituted in MSP1D1 nanodiscs. (F) SEC of NK1R[2–335] in nanodiscs, using Superdex 200 Increase 10/300 GL column, with monitoring of the ultraviolet

absorption at 280 nm. NK1R[2–335] contains the additional N-terminal residues GP and the additional C-terminal residues ENLYFQ from the two cleavage sites.

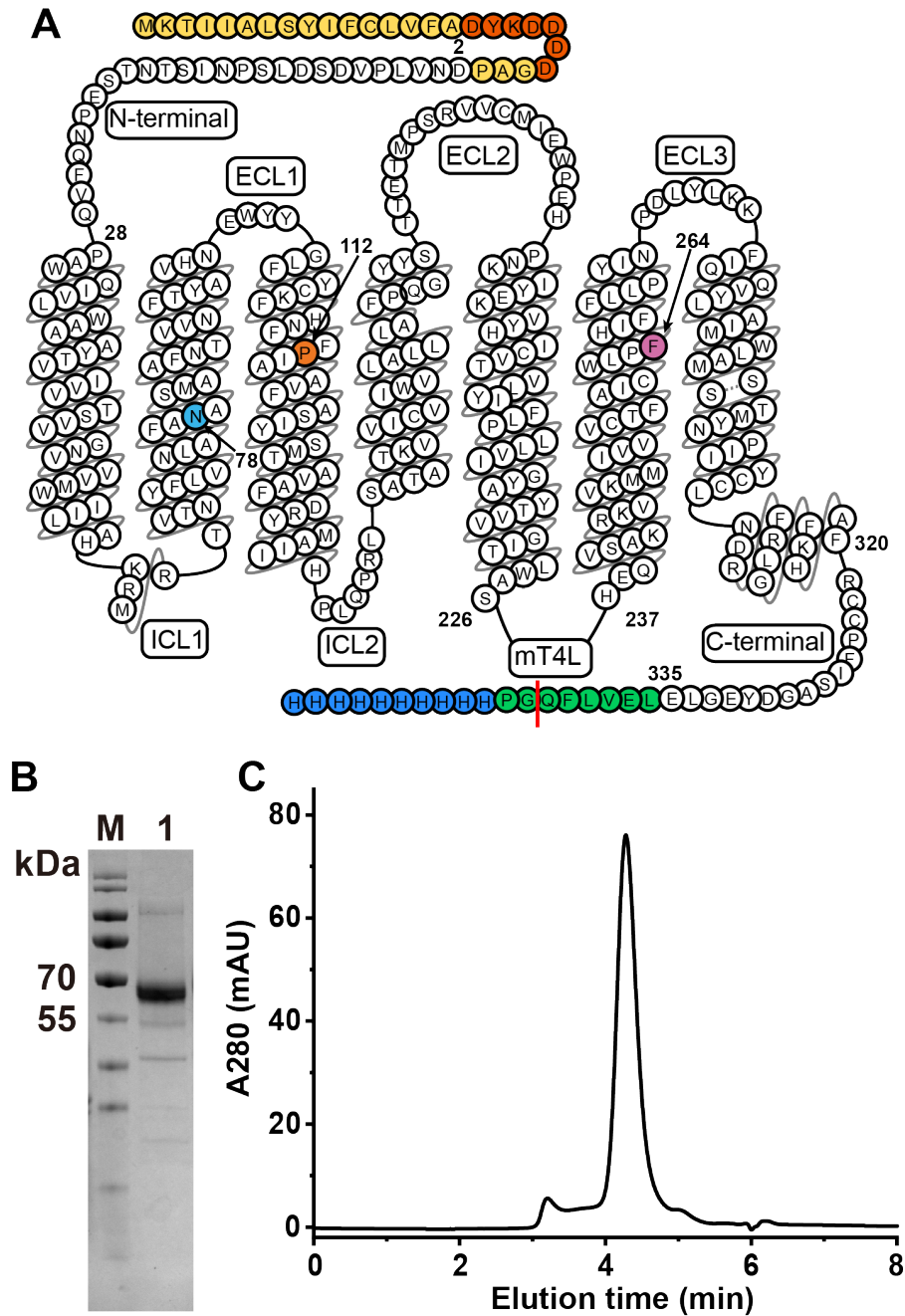


Fig. S2. NK1R[2–335, E78^{2.50N}]-mT4L expression in Sf9 insect cells. (A) Schematic diagram of the NK1R construct used (Modified from GPCRdb). Modified T4 lysozyme (mT4L) was inserted between the residues S226 and H237 of the third intracellular loop. A cyan ball indicates the location of the engineered mutation E78^{2.50N}; an orange ball indicates the P112^{3.32} position and a purple ball indicates the F264^{6.51} position. The red line shows the PPase digestion site. (B) SDS-PAGE of purified NK1R[2–335, E78^{2.50N}]-mT4L. (C) aSEC of NK1R[2–335, E78^{2.50N}]-mT4L in complex with the antagonist aprepitant in DDM/CHS mixed micelles.

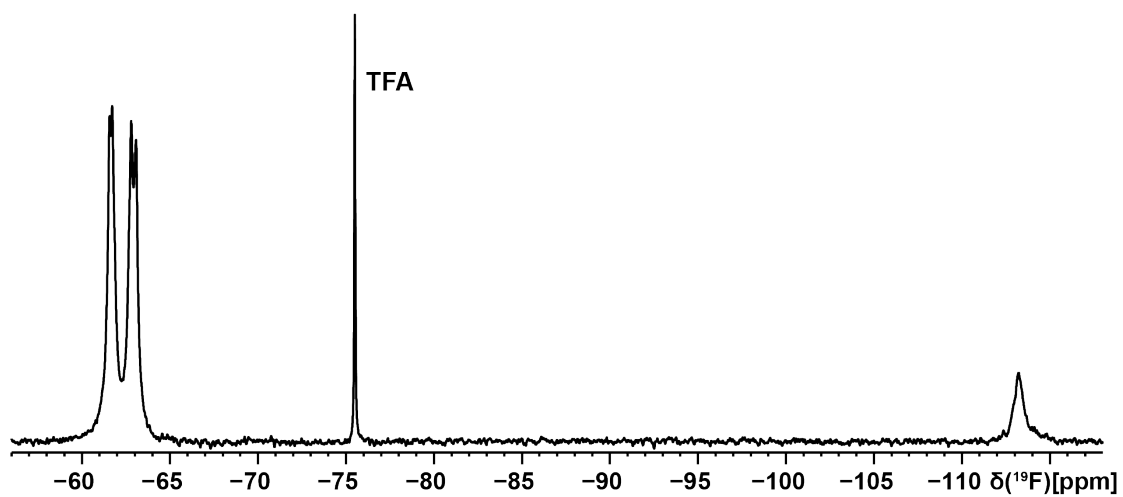


Fig. S3. Complete 1D ^{19}F -NMR spectra of aprepitant in complex with NK1R[2–335]. The spectral region from -60 ppm to -64 ppm shows the resonances of the trifluoromethyl groups of the bis-trifluoromethyl-phenylethoxy moiety (Fig. 1C). The spectral region from -112 ppm to -115 ppm shows the resonances of the 4-fluorophenyl moiety (Fig. 1C), and the resonances at -75.5 ppm represents the internal reference TFA.

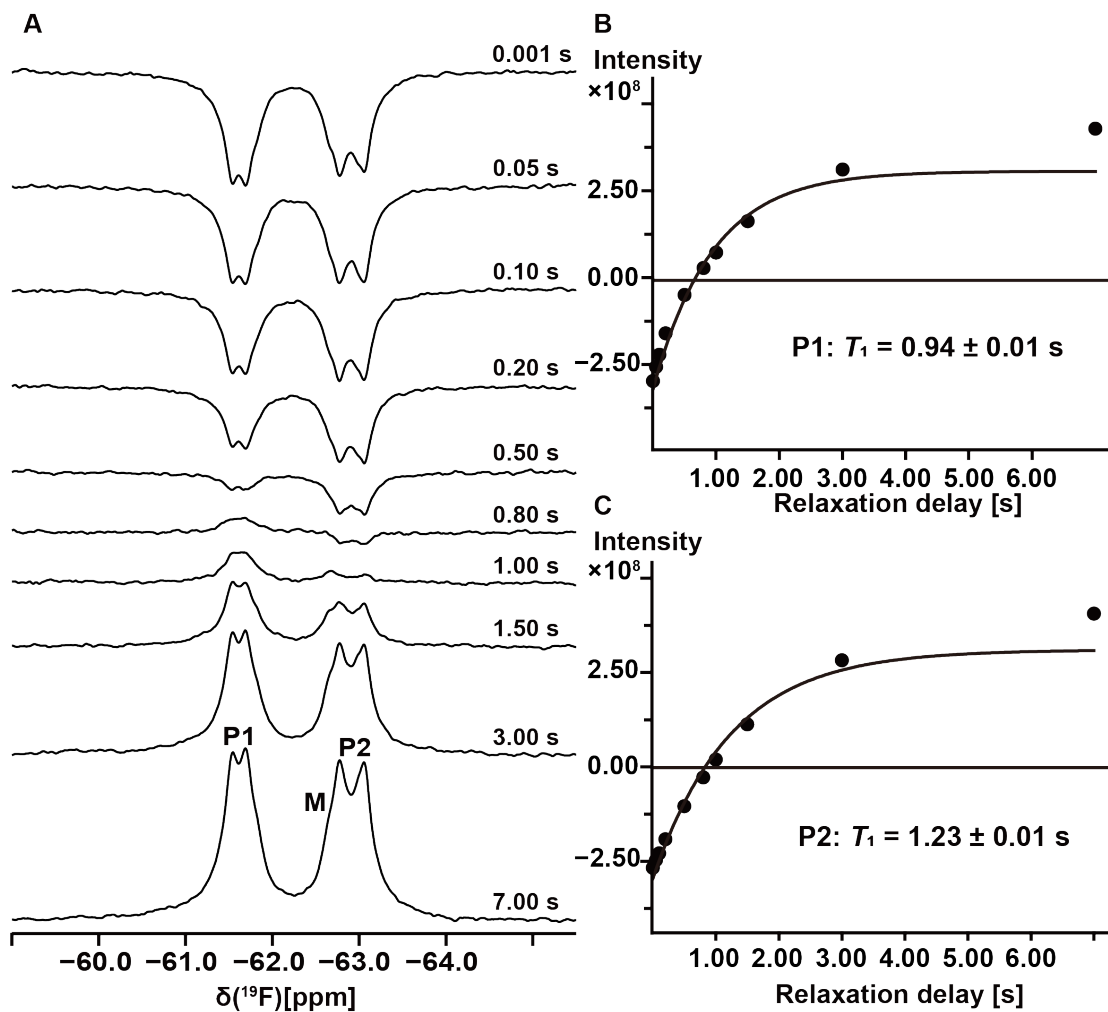


Fig. S4. Longitudinal ^{19}F spin relaxation time (T_1) of aprepitant bound to NK1R[2–335] in LMNG/CHS micelles at 298 K. (A) Inversion recovery NMR experiment. The recovery delays are indicated on the right above the spectra. The spectra were recorded with accumulation of 512 scans per increment, the sample concentration was 200 μM . (B) Plots of the signal intensities of P1 and P2 versus the relaxation delays. (see *SI Text*). The fitted T_1 relaxation times for P1 and P2 are indicated below the horizontal line at 0.00 intensity.

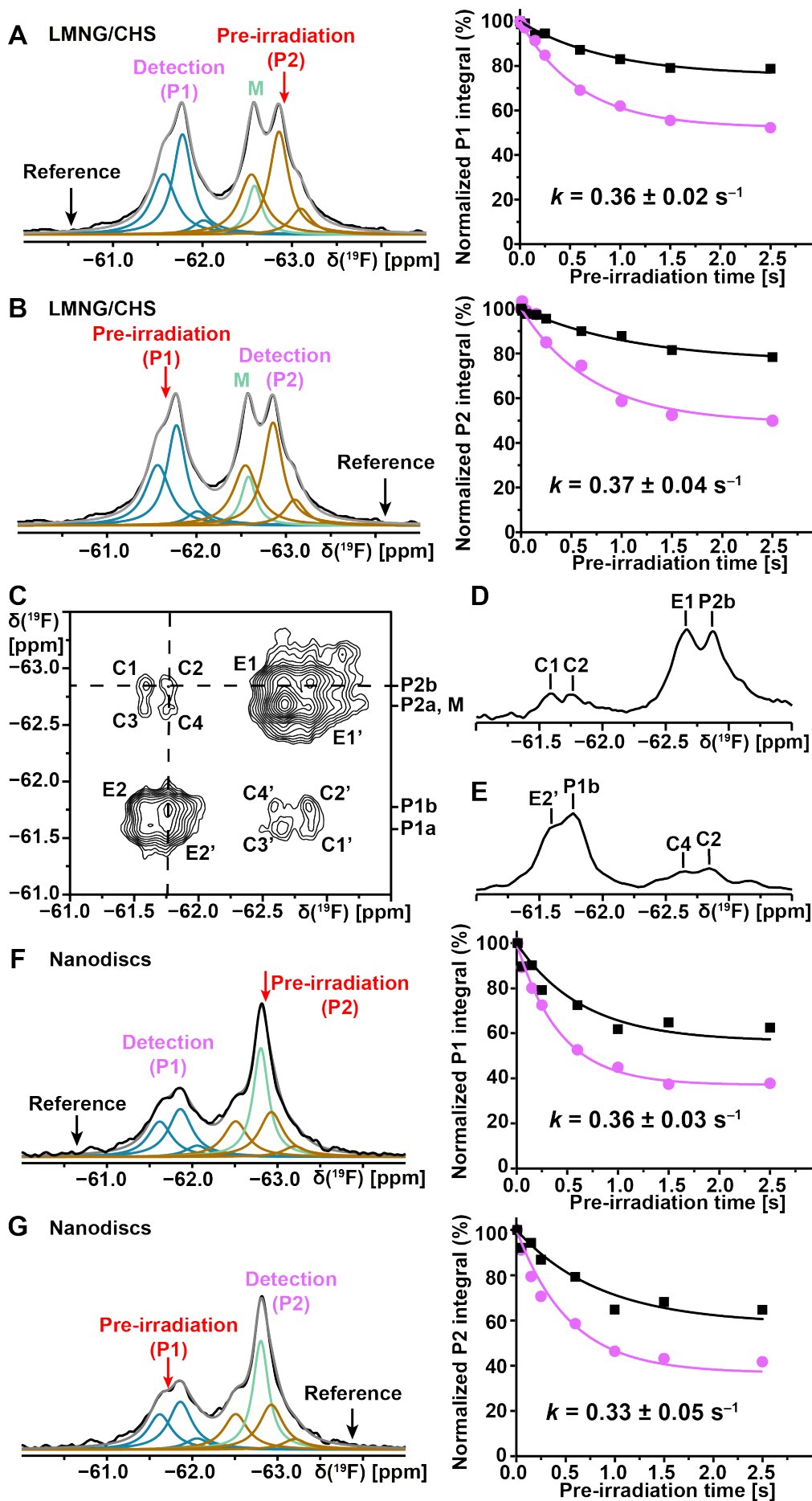


Fig. S5. Large-amplitude structure fluctuations in NK1R[2–335, E78^{2.50}N] detected by ¹⁹F-NMR observation of the bound drug aprepitant at 298 K. NK1R[2–335, E78^{2.50}N] was expressed in *Pichia pastoris*. (A) and (B) Saturation transfer ¹⁹F-NMR experiments with NK1R[2–335, E78^{2.50}N] in mixed micelles of LMNG and CHS. In each experiment, the red arrow indicates the carrier positions for the pre-irradiation, the black arrow indicates the position of the reference irradiation, the detection position is indicated with purple lettering. Lorentzian deconvolution of the 1D ¹⁹F-NMR spectra is used to identify a minimal number of overlapping signals that provide a quantitative fit of the experimental spectrum. The plots on the right show the normalized integrals of the observed peak at variable pre-irradiation times on-resonance (purple) and at the reference positions (black). The Bloch–McConnell equation was used to fit the experimental data and derive the exchange rates. (C) 2D [¹⁹F, ¹⁹F]-EXSY spectrum of NK1R[2–335, E78^{2.50}N] in mixed micelles of LMNG and CHS at 298 K, mixing time = 600 ms. The positions of the diagonal peaks P1, M and P2 are indicated on the right. The cross peaks C and C' represent the exchange between P1 and P2, where exchange between pairs of substates is manifested by the fine structures C1 to C4 and C1' to C4' (see text). The cross peaks E1, E1', E2 and E2' represent exchange among substates within the manifolds of P1 and P2. (D) 1D cross section along the dashed horizontal line in (C). (E) 1D cross section along the dashed vertical line in (C). (F) and (G) Same experiments and same presentation as in (A) and (B) for NK1R[2–335, E78^{2.50}N] in nanodiscs.

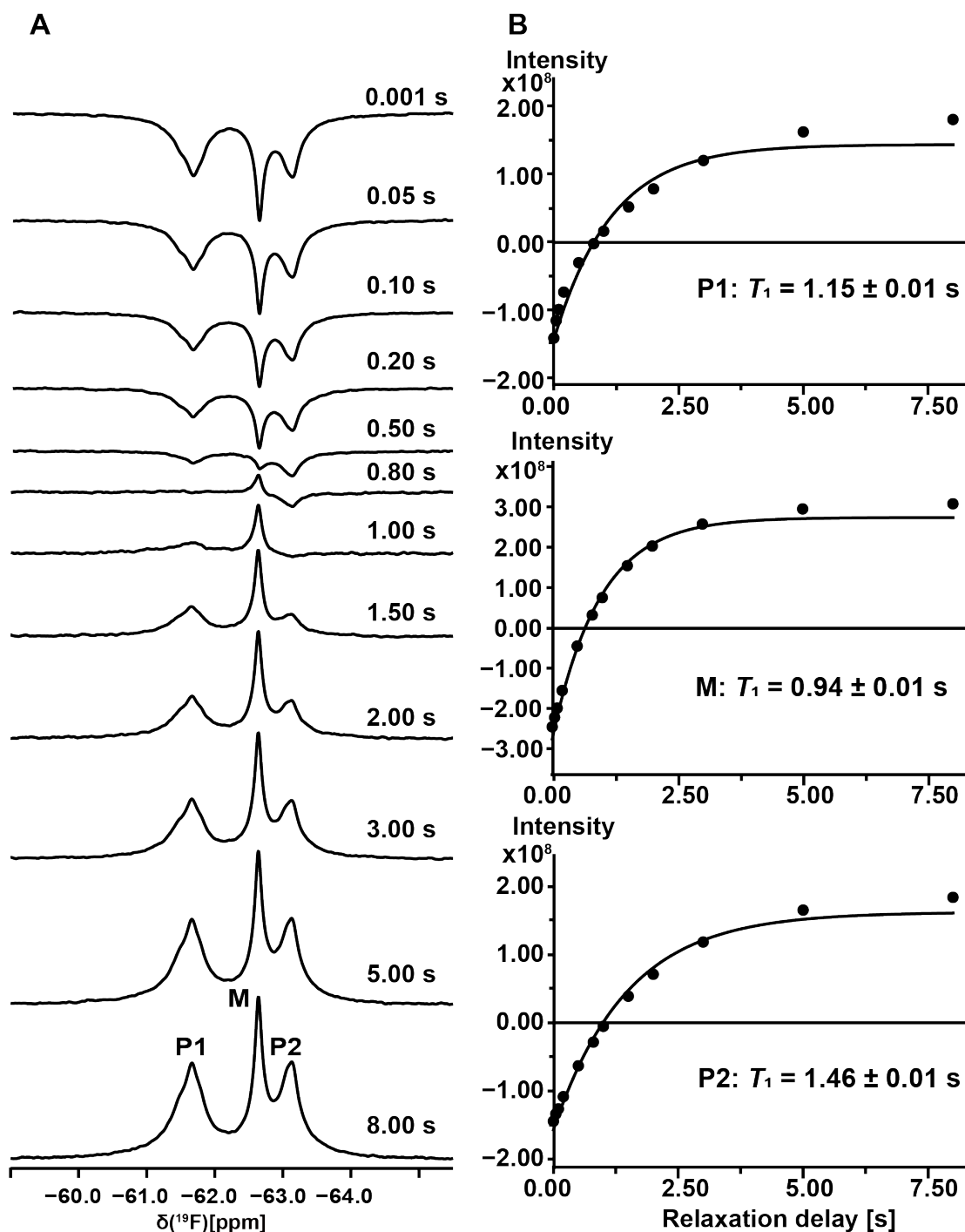
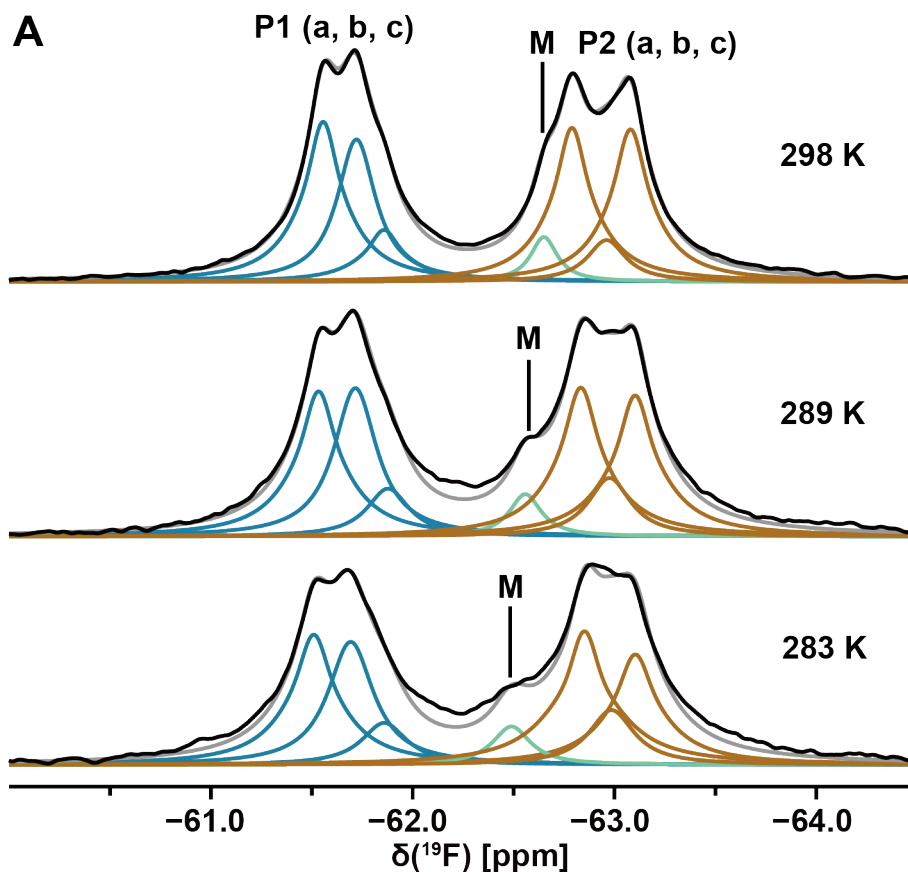


Fig. S6. Longitudinal ^{19}F spin relaxation time (T_1) of aprepitant bound to NK1R[2–335, E782-50N] in DDM/CHS micelles. (A) Inversion recovery NMR experiment. The recovery delays are indicated on the right above of the spectra. The spectra were recorded at 298 K with accumulation of 2,048 scans per increment, the sample concentration was 100 μM . (B) Plots of the signal intensities of P1, M, and P2 versus the relaxation delays (see *SI Text*); the fitted T_1 relaxation times are indicated below the horizontal line at 0.00 intensity.



B

Lorentzian deconvolution of ^{19}F -NMR spectra

Peak	289 K		283 K	
	Chemical shift (ppm)	Line width (Hz)	Chemical shift (ppm)	Line width (Hz)
P1a	-61.53	145	-61.51	150
P1b	-61.71	146	-61.69	154
P1c	-61.89	143	-61.86	153
M	-62.56	108	-62.49	128
P2a	-62.83	145	-62.85	155
P2b	-63.10	145	-63.10	152
P2c	-62.98	144	-62.99	153

Fig. S7. Temperature dependence of the ^{19}F -NMR spectra of the NK1R–aprepitant complex in LMNG/CHS mixed micelles. (A) 1D ^{19}F -NMR spectra of the NK1R[2–335]–aprepitant complex at 298 K, 289 K and 283 K. Chemical shifts were referenced to TFA at -75.5 ppm. Lorentzian deconvolution of the ^{19}F -NMR signals is shown in blue (P1) and brown (P2). (B) ^{19}F chemical shifts and line widths of the selected spectra shown in (A).

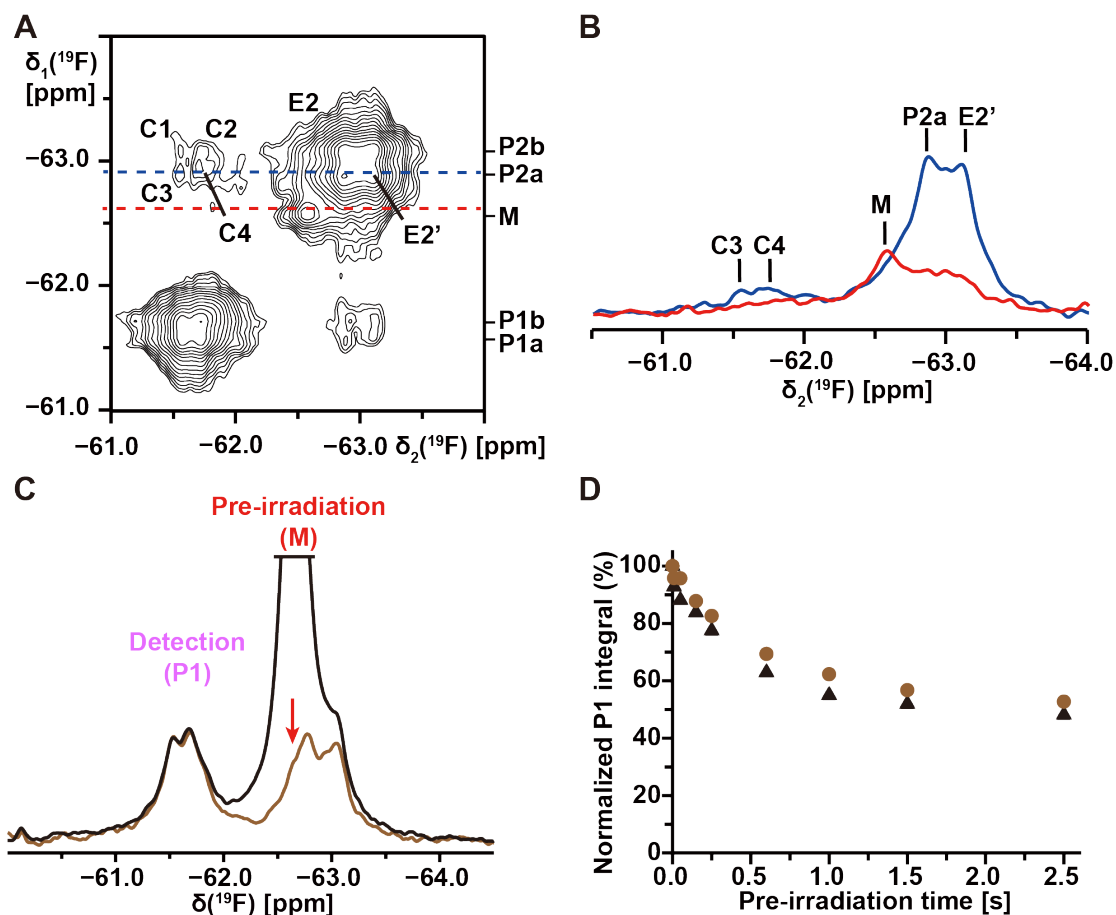


Fig. S8. Exchange of micelle-bound aprepitant with protein-bound aprepitant is too slow to be seen in the experiments used in this paper. (A) 2D [^{19}F , ^{19}F]-EXSY spectrum of NK1R[2–335] in mixed micelles of LMNG and CHS at 289 K, mixing time = 600 ms. (B) 1D cross sections along the dashed horizontal blue and red lines in (A). (C) 1D ^{19}F -NMR spectra recorded with pre-irradiation at the position of the signal of free aprepitant (M) at two different concentrations of the ligand. NK1R[2–335], concentration = 36 μM , T = 298 K. Brown line, 40 μM aprepitant; Black line, 80 μM aprepitant. (D) Plots of the normalized integrals of the observed peak P1 at different pre-irradiation times for the two different aprepitant concentrations.

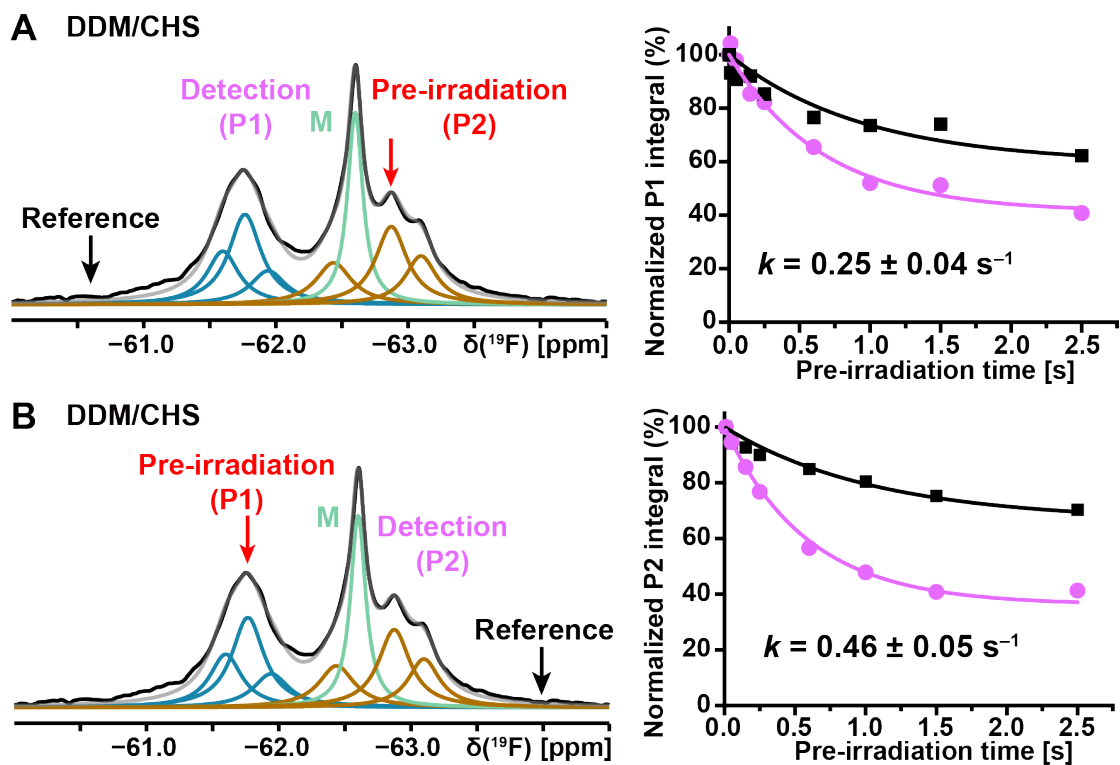


Fig. S9. Large-amplitude structure fluctuations of NK1R[2–335, E78^{2.50}N] in DDM/CHS micelles at 298 K detected by ¹⁹F-NMR observation of the bound drug aprepitant. (A) and (B) Saturation transfer ¹⁹F-NMR experiments with observation of the trifluoromethyl groups of aprepitant. Same presentation as in Fig. 2.

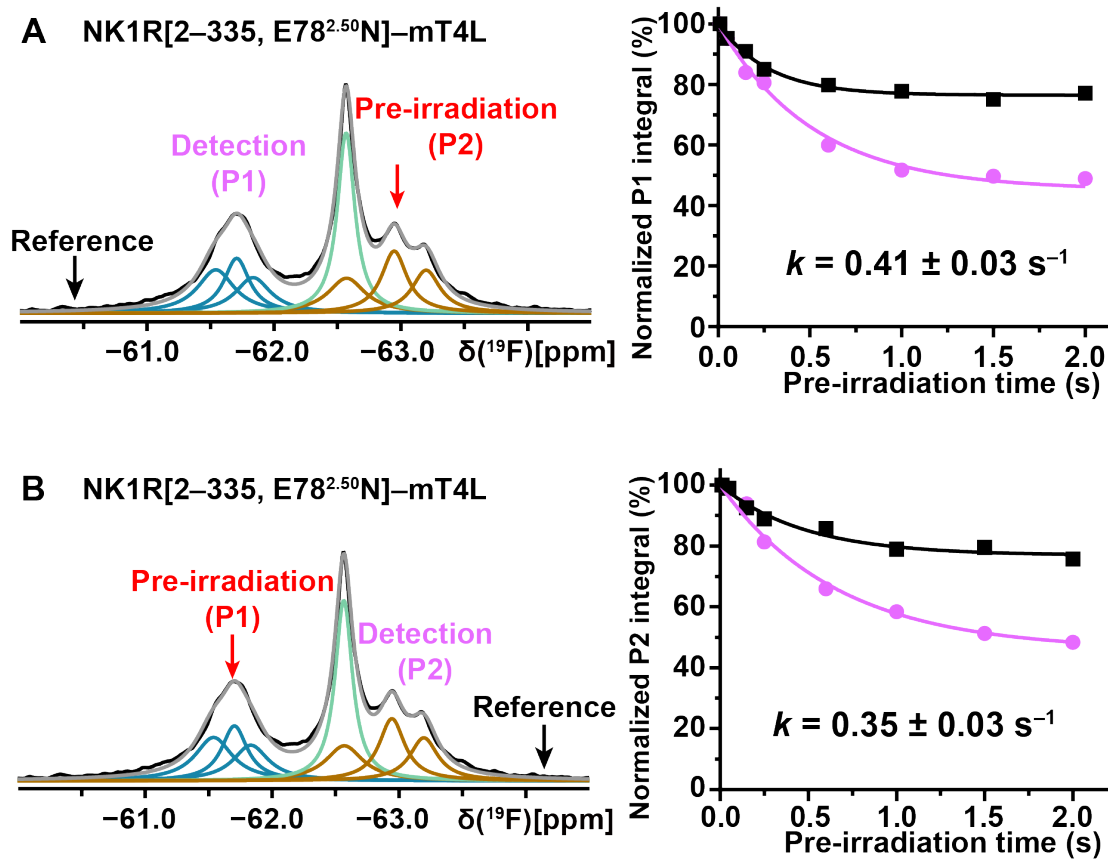


Fig. S10. Large-amplitude structure fluctuations of NK1R[2–335, E78^{2.50}N]–mT4L in DDM/CHS micelles at 298 K detected by ¹⁹F-NMR observation of the bound drug aprepitant. (A) and (B) ¹⁹F-NMR saturation transfer between the trifluoromethyl groups of aprepitant. Same presentation as in Fig. 2.

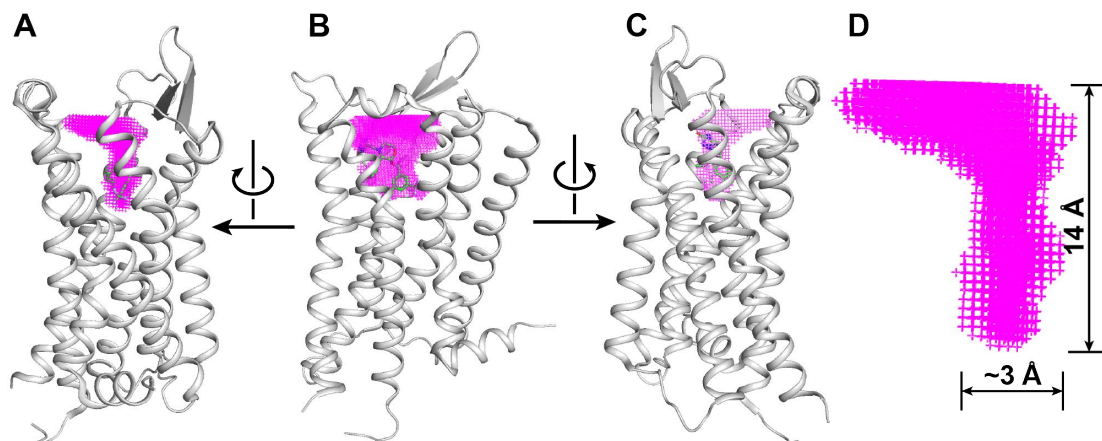


Fig. S11. Shape and size of the orthosteric binding groove of NK1R. (A–C) Crystal structure of the NK1R–aprepitant complex (PDB: 6J20). NK1R is shown in grey ribbon presentation. Aprepitant is shown in green stick presentation inside the binding groove. The binding groove generated by the program POCASA (8) is shown in magenta. (A) and (C) are views derived from (B) by -90 degree and $+90$ degree rotations about a vertical axis, respectively. (D) Indication of the dimensions of the binding groove in (A) to (C).

Table S1. Lorentzian deconvolution of ^{19}F -NMR spectra at 298 K of NK1R[2–335] and NK1R[2–335, E78 $^{2.50}\text{N}$] reconstituted in different micelles and in nanodiscs

NK1R[2–335] in LMNG/CHS	P1a	P1b	P1c	M	P2a	P2b	P2c
Chemical shift (ppm) ^a	-61.6	-61.7	-61.9	-62.6	-62.8	-63.1	-63.0
Line width (Hz) ^b	133	130	131	91	131	133	130
Integral (%) ^c	22.6	18.2	7.2	4.0	21.4	21.3	5.3
Total (%) ^d		48.0		4.0		48.0	

NK1R[2–335] in nanodiscs	P1a	P1b	P1c	M	P2a	P2b	P2c
Chemical shift (ppm) ^a	-61.5	-61.7	-61.9	-62.9	-62.6	-63.0	-63.1
Line width (Hz) ^b	182	184	183	120	183	183	183
Integral (%) ^c	11.5	21.1	9.6	17.6	10.6	20.8	8.8
Total (%) ^d		42.2		17.6		40.2	

NK1R[2–335, E78 $^{2.50}\text{N}$] in LMNG/CHS	P1a	P1b	P1c	M	P2a	P2b	P2c
Chemical shift (ppm) ^a	-61.6	-61.8	-62.1	-62.6	-62.5	-63.0	-63.1
Line width (Hz) ^b	185	145	157	110	185	145	156
Integral (%) ^c	17.6	22.9	3.6	8.5	17.5	23.5	6.4
Total (%) ^d		44.1		8.5		47.4	

NK1R[2–335, E78 ^{2.50} N] in DDM/CHS	P1a	P1b	P1c	M	P2a	P2b	P2c
Chemical shift (ppm) ^a	-61.6	-61.8	-61.9	-62.6	-62.5	-62.9	-63.1
Line width (Hz) ^b	166	167	184	79	184	163	162
Integral (%) ^c	12.0	20.5	8.5	20.5	10.5	17.3	10.7
Total (%) ^d		41.0		20.5		38.5	

NK1R[2–335, E78 ^{2.50} N] in nanodiscs	P1a	P1b	P1c	M	P2a	P2b	P2c
Chemical shift (ppm) ^a	-61.6	-61.9	-62.1	-62.8	-62.5	-62.9	-63.2
Line width (Hz) ^b	190	189	185	123	192	190	190
Integral (%) ^c	13.8	18.6	4.3	27.5	14.1	17.5	4.2
Total (%) ^d		36.7		27.5		35.8	

^a Chemical shift was referenced to trifluoromethyl acetic acid to -75.5 ppm.

^b Lorentzian deconvolution was used to identify a minimal number of overlapping signals that provide a quantitative fit of the experimental spectrum.

^c Percentage of the integrated peak intensity relative to the total trifluoromethyl signal from -58.0 to -66.0 ppm.

^d Total integrated intensities of P1, M and P2, respectively.

SI References:

1. M. T. Eddy *et al.*, Allosteric coupling of drug binding and intracellular signaling in the A_{2A} adenosine receptor. *Cell* **172**, 68-80 e12 (2018).
2. M. T. Eddy *et al.*, Extrinsic tryptophans as NMR probes of allosteric coupling in membrane proteins: application to the A_{2A} adenosine receptor. *J. Am. Chem. Soc.* **140**, 8228-8235 (2018).
3. S. Chen *et al.*, Human substance P receptor binding mode of the antagonist drug aprepitant by NMR and crystallography. *Nat. Commun.* **10**, 638 (2019).
4. T. K. Ritchie *et al.*, Chapter 11-Reconstitution of membrane proteins in phospholipid bilayer nanodiscs. *Methods Enzymol.* **464**, 211-231 (2009)
5. C. L. Perrin, T. J. Dwyer, Application of two-dimensional NMR to kinetics of chemical exchange. *Chem. Rev.* **90**, 935-967 (1990).
6. S. Forsén, R. A. Hoffman, Exchange rates by nuclear magnetic multiple resonance. III. exchange reactions in systems with several nonequivalent sites. *J. Chem. Phys.* **40**, 1189-1196 (1964).
7. S. Forsén, R. A. Hoffman, Study of moderately rapid chemical exchange reactions by means of nuclear magnetic double resonance. *J. Chem. Phys.* **39**, 2892-2901 (1963).
8. J. Yu, Y. Zhou, I. Tanaka, M. Yao, Roll: a new algorithm for the detection of protein pockets and cavities with a rolling probe sphere. *Bioinformatics* **26**, 46-52 (2010).